



On the linear stability of eccentrically stiffened functionally graded annular spherical shell on elastic foundations

Vu Thi Thuy Anh, Pham Hong Cong, Dao Huy Bich & Nguyen Dinh Duc

To cite this article: Vu Thi Thuy Anh, Pham Hong Cong, Dao Huy Bich & Nguyen Dinh Duc (2016): On the linear stability of eccentrically stiffened functionally graded annular spherical shell on elastic foundations, *Advanced Composite Materials*, DOI: [10.1080/09243046.2016.1187819](https://doi.org/10.1080/09243046.2016.1187819)

To link to this article: <http://dx.doi.org/10.1080/09243046.2016.1187819>



Published online: 13 Jun 2016.



Submit your article to this journal [↗](#)



View related articles [↗](#)



View Crossmark data [↗](#)

On the linear stability of eccentrically stiffened functionally graded annular spherical shell on elastic foundations

Vu Thi Thuy Anh, Pham Hong Cong, Dao Huy Bich and Nguyen Dinh Duc*

University of Engineering and Technology, Vietnam National University, Hanoi – 144, Xuan Thuy – Cau Giay, Hanoi, Vietnam

(Received 9 April 2015; accepted 14 June 2015)

The study deals with the formulation of governing equations of eccentrically stiffened functionally graded materials annular spherical shells resting on elastic foundations and based upon the classical shell theory and the smeared stiffeners technique taking into account geometrical nonlinearity in Von Karman-Donnell sense. The annular spherical shells are reinforced by eccentrically longitudinal and transversal stiffeners made of full metal or full ceramic depending on situation of stiffeners at metal-rich side or ceramic-rich side of the shell respectively. Approximate solutions are assumed to satisfy the simply supported boundary condition and Galerkin method is applied to obtain closed-form relations of bifurcation type of buckling loads. Numerical results are given to evaluate effects of inhomogeneous, dimensional parameters, outside stiffeners and elastic foundations to the buckling of structures.

Keywords: linear stability; FGM annular spherical shells; eccentrically stiffened; elastic foundations

1. Introduction

Shells have increased structural stiffness compared to plates. The advantage of shell structures is their capability of carrying loads and moments by a combined membrane and bending action due to their curvature. On the other hand, advanced composite or functionally graded materials (FGM) provide high-performance and reliability due to their well-known characteristics. As a result, shell structures made of FGM will continue being widely used for many years in various engineering fields such as naval, aerospace, auto-motive, industrial constructions and for sporting goods, medical devices and many other areas. Moreover, the FGM shells, as other composite structures, usually reinforced by stiffening members to provide the benefit of added – load-carrying static and dynamic capability with a relatively small additional weight penalty. In other words, in order to provide material continuity and ease of manufacture, the FGM shells are reinforced by an eccentrically homogeneous stiffener system. To date, the investigation on statics and dynamics of eccentrically stiffened shell structures made of FGM have received comparatively little attention. Najafizadeh et al. [1] studied linear static buckling of FGM axially loaded cylindrical shell reinforced by ring and stringer FGM stiffeners. Bich et al. studied nonlinear post-buckling and dynamics of eccentrically stiffened functionally graded shallow shells and panels.[2,3] Dung and Hoa [4,5] presented an analytical study of nonlinear static buckling and post-buckling analysis of

*Corresponding author. Email: ducnd@vnu.edu.vn

eccentrically stiffened functionally graded circular cylindrical shells under external pressure and torsional load with FGM stiffeners and approximate three-term solution of deflection taking into account the nonlinear buckling shape. Recently, Duc et al. [6–11] have published several studies on the eccentrically stiffened shell structures made of FGM under mechanical and thermal loads; for example, they investigated nonlinear dynamic response of imperfect eccentrically stiffened doubly curved FGM shallow shells on elastic foundations,[6] presented nonlinear post-buckling of imperfect eccentrically stiffened FGM double-curved thin shallow shells in thermal environments,[7] studied nonlinear response of imperfect eccentrically stiffened ceramic-metal-ceramic FGM circular cylindrical shells surrounded by elastic foundations and subjected to axial compression.[11]

Notice that in all the publications mentioned above, the shell structures are mainly concentrated in the common form, while nowadays, with the development of esthetics, architecture and design are becoming diversified and abundant, the special shapes of the spherical shells more widely used in practical applications. In which, the annular spherical shell is one of the special shapes of the spherical shells. Despite the evident importance in practical applications, it is a fact from the open literature that investigations on the thermo-elastic, dynamic and buckling analysis of FGM annular spherical shell is comparatively scarce. The most difficult part in annular shell problems is complex calculations.

Can enumerate some studies of annular spherical shells as Alwar and Narasimhan [12] investigated the axisymmetric nonlinear analysis of laminated orthotropic annular spherical shells, the object of this investigation is to give analytical solutions of large axisymmetric deformation of laminated orthotropic spherical shells including asymmetric laminates. Wu and Tsai [13] studied the asymptotic differential quadrature (DQ) solutions of functionally graded annular spherical shells by combining the method of DQ with the asymptotic expansion approach. Most recently, Anh et al. [14] analyzed the nonlinear buckling analysis of thin FGM annular spherical shells on elastic foundations under external pressure and thermal loads. Bich and Phuong [15] investigated the buckling analysis of FGM annular spherical shells and segments subjected to compressive load and radial pressure.

In this paper, the linear analysis of eccentrically stiffened FGM annular spherical shell is investigated. The shells are reinforced by eccentrically longitudinal and transverse stiffeners made of full metal or full ceramic depending on situation of stiffeners on the metal-rich side or ceramic-rich side of the shell, respectively. Approximate solutions are assumed to satisfy the simply supported boundary condition and Galerkin method is applied to obtain closed-form relations of bifurcation type of buckling loads. The paper analyzed and discussed the effects of material and geometrical properties, elastic foundations and eccentric stiffeners on the buckling load of the eccentrically stiffened FGM annular spherical shell.

2. Functionally graded annular spherical shell and elastic foundation

Consider an annular spherical shell made of FGM with radius of curvature R , rise H (H is the distance from the bottom plane of annular spherical shell with radius r_1 to the peak of the spherical shell, from which is creating the annular spherical shell), radii of lower and upper bases r_1 , r_0 respectively and thickness h . The FGM annular spherical shell reinforced by eccentrically longitudinal and transverse stiffeners is shown in Figure 1.

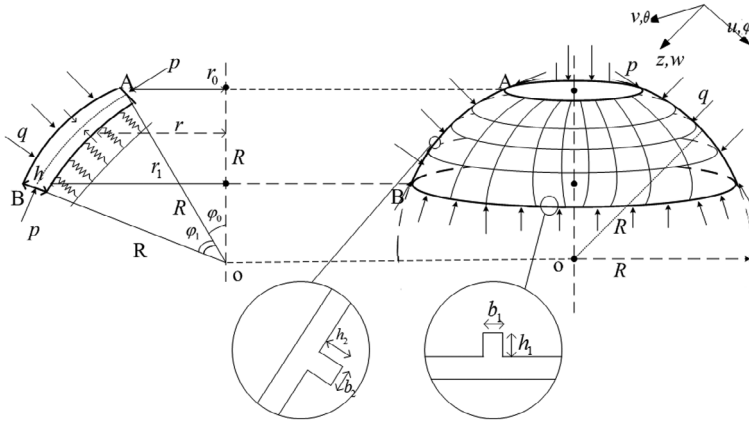


Figure 1. Configuration of the eccentrically stiffened FGM annular spherical shell.

The annular spherical shell is made from a mixture of ceramics and metals, and is defined in coordinate system (φ, θ, z) , where φ and θ are in the meridional and circumferential directions of the shells, respectively and z is perpendicular to the middle surface, positive inward.

Suppose that the material composition of the shell varies smoothly along the thickness by a simple power law in terms of the volume fractions of the constituents as

$$V_c(z) = \left(\frac{2z+h}{2h}\right)^k, \quad -\frac{h}{2} \leq z \leq \frac{h}{2}, \quad (1)$$

$$V_m(z) = 1 - V_c(z).$$

where k (volume fraction index) is a non-negative number that defines the material distribution, subscripts m and c represent the metal and ceramic constituents, respectively.

The effective properties of FGM shallow spherical shell such as modulus of elasticity, the coefficient of thermal expansion, the coefficient of thermal conduction of FGM annular spherical shell can be defined as:

$$E(z) = E_m + E_{cm} \left(\frac{2z+h}{2h}\right)^k, \quad -\frac{h}{2} \leq z \leq \frac{h}{2}. \quad (2)$$

the Poisson ratio ν is assumed to be constant $\nu(z) = \text{const}$ and $E_{cm} = E_c - E_m$.

The reaction–deflection relation of Pasternak foundation is given by [14]:

$$q_e = k_1 w - k_2 \Delta w$$

where $\Delta w = \frac{\partial^2 w}{\partial r^2} + \frac{1}{r} \frac{\partial w}{\partial r} + \frac{1}{r^2} \frac{\partial^2 w}{\partial \theta^2}$ is a Laplace’s operator, w is the deflection of the annular spherical shell, k_1 is Winkler foundation modulus, and k_2 is the shear layer foundation stiffness of Pasternak model.

3. Theoretical formulations and stability analysis

In the present study, the classical shell theory is used to obtain the equilibrium and compatibility equations as well as expressions of buckling loads and nonlinear load–deflection curves of thin FGM annular spherical shells. For a thin annular spherical shell it is convenient to introduce a variable r ; referred as the radius of parallel circle

with the base of shell and defined by $r = R \sin \varphi$. Moreover, due to shallowness of the shell it is approximately assumed that $\cos \varphi = 1$, $Rd\varphi = dr$.

According to the classical shell theory, the strains at the middle surface and the change of curvatures and twist are related to the displacement components u, v, w in the φ, θ, z coordinate directions, respectively, taking into account Von Karman–Donnell nonlinear terms as [14,15]:

$$\begin{aligned} \varepsilon_r^0 &= \frac{\partial u}{\partial r} - \frac{w}{R} + \frac{1}{2} \left(\frac{\partial w}{\partial r} \right)^2, & \chi_r &= \frac{\partial^2 w}{\partial r^2}, \\ \varepsilon_\theta^0 &= \frac{1}{r} \left(\frac{\partial v}{\partial \theta} + u \right) - \frac{w}{R} + \frac{1}{2r^2} \left(\frac{\partial w}{\partial \theta} \right)^2, & \chi_\theta &= \frac{1}{r} \frac{\partial w}{\partial r} + \frac{1}{r^2} \frac{\partial^2 w}{\partial \theta^2}, \\ \gamma_{r\theta}^0 &= \frac{\partial v}{\partial r} + \frac{1}{r} \frac{\partial u}{\partial \theta} - \frac{v}{r} + \frac{1}{r} \frac{\partial w}{\partial r} \frac{\partial w}{\partial \theta}, & \chi_{r\theta} &= \frac{1}{r} \frac{\partial^2 w}{\partial r \partial \theta} - \frac{1}{r^2} \frac{\partial w}{\partial \theta}. \end{aligned} \quad (3)$$

where ε_r^0 and ε_θ^0 are the normal strains, $\gamma_{r\theta}^0$ is the shear strain at the middle surface of the spherical shell, $\chi_r, \chi_\theta, \chi_{r\theta}$ are the changes of curvatures and twist.

The nonlinear equilibrium equations of a perfect shallow spherical shell based on the classical shell theory are: [14,15]

$$\frac{\partial N_r}{\partial r} + \frac{1}{r} \frac{\partial N_{r\theta}}{\partial \theta} + \frac{N_r}{r} - \frac{N_\theta}{r} = 0, \quad (4)$$

$$\frac{\partial N_\theta}{r \partial \theta} + \frac{\partial N_{r\theta}}{\partial r} + \frac{2N_{r\theta}}{r} = 0, \quad (5)$$

$$\begin{aligned} & \frac{\partial^2 M_r}{\partial r^2} + \frac{2}{r} \frac{\partial M_r}{\partial r} + 2 \left(\frac{\partial^2 M_{r\theta}}{r \partial r \partial \theta} + \frac{1}{r^2} \frac{\partial M_{r\theta}}{\partial \theta} \right) + \frac{1}{r^2} \frac{\partial^2 M_\theta}{\partial \theta^2} - \frac{1}{r} \frac{\partial M_\theta}{\partial r} + \frac{1}{R} (N_r + N_\theta) \\ & + N_r \frac{\partial^2 w}{\partial r^2} - 2N_{r\theta} \left(\frac{1}{r} \frac{\partial w}{\partial \theta} - \frac{\partial^2 w}{r \partial r \partial \theta} \right) + N_\theta \left(\frac{1}{r} \frac{\partial w}{\partial r} + \frac{1}{r^2} \frac{\partial^2 w}{\partial \theta^2} \right) + q - k_1 w + k_2 \Delta w = 0. \end{aligned} \quad (6)$$

The force and moment resultants of an FGM annular spherical shell are:

$$\begin{aligned} N_r &= \left(A_{11} + \frac{E_0 A_1}{s_1} \right) \varepsilon_r^0 + A_{12} \varepsilon_\theta^0 - (B_{11} + C_1) \chi_r - B_{12} \chi_\theta, \\ N_\theta &= A_{12} \varepsilon_r^0 + \left(A_{22} + \frac{E_0 A_2}{s_2} \right) \varepsilon_\theta^0 - B_{12} \chi_r - (B_{22} + C_2) \chi_\theta, \\ N_{r\theta} &= A_{66} \gamma_{r\theta}^0 - 2B_{66} \chi_{r\theta}, \quad M_r = (B_{11} + C_1) \varepsilon_r^0 + B_{12} \varepsilon_\theta^0 - \left(D_{11} + \frac{E_0 I_1}{s_1} \right) \chi_r - D_{12} \chi_\theta, \\ M_\theta &= B_{12} \varepsilon_r^0 + (B_{22} + C_2) \varepsilon_\theta^0 - D_{12} \chi_r - \left(D_{22} + \frac{E_0 I_2}{s_2} \right) \chi_\theta, \\ M_{r\theta} &= B_{66} \gamma_{r\theta}^0 - 2D_{66} \chi_{r\theta}, \end{aligned} \quad (7)$$

Where,

$$\begin{aligned} A_{11} &= A_{22} = \frac{E_1}{1-\nu^2}; & A_{12} &= \frac{E_1 \nu}{1-\nu^2}; & A_{66} &= \frac{E_1}{2(1+\nu)}; & C_1 &= \frac{E_0 A_1 z_1}{s_1}; & C_2 &= \frac{E_0 A_2 z_2}{s_2}; \\ B_{11} &= B_{22} = \frac{E_2}{1-\nu^2}; & B_{12} &= \frac{E_2 \nu}{1-\nu^2}; & B_{66} &= \frac{E_2}{2(1+\nu)}; & I_1 &= \frac{d_1 h^3}{12} + A_1 z_1^2; & z_1 &= \frac{h_1+h}{2}; \\ D_{11} &= D_{22} = \frac{E_3}{1-\nu^2}; & D_{12} &= \frac{E_3 \nu}{1-\nu^2}; & D_{66} &= \frac{E_3}{2(1+\nu)}; & I_2 &= \frac{d_2 h^3}{12} + A_2 z_2^2; & z_2 &= \frac{h_2+h}{2}; \\ s_1 &= \frac{2\pi r}{n_1}, & s_2 &= \frac{R\varphi_1 - R\varphi_0}{n_2} = \frac{R}{n_2} \left(\arcsin \frac{r_1}{R} - \arcsin \frac{r_0}{R} \right). \end{aligned} \quad (8)$$

where s_1, s_2 – the distance between eccentrically longitudinal and transverse stiffeners respectively. A_1, A_2 – the cross-sectional area of eccentrically longitudinal and latitude

stiffeners, respectively. d_1 , d_2 and h_1 , h_2 – the width and height of eccentrically longitudinal and latitude stiffeners, respectively. n_1 , n_2 – the numbers of eccentrically longitudinal and latitude stiffeners respectively, and E_0 – Young’s modulus of the stiffeners. $E_0 = E_c$ if the stiffeners are reinforced on the surface of the ceramic-rich side, $E_0 = E_m$ if the stiffeners are reinforced on the surface of the metal-rich.

$$\begin{aligned} E_1 &= \int_{-h/2}^{h/2} \left[E_c + E_{cm} \left(\frac{2z+h}{h} \right)^k \right] dz = hE_m + \frac{hE_{cm}}{k+1}, \\ E_2 &= \int_{-h/2}^{h/2} z \left[E_c + E_{cm} \left(\frac{2z+h}{h} \right)^k \right] dz = h^2 E_{cm} \left(\frac{1}{k+2} - \frac{1}{2k+2} \right), \\ E_3 &= \int_{-h/2}^{h/2} z^2 \left[E_c + E_{cm} \left(\frac{2z+h}{h} \right)^k \right] dz = \frac{h^3 E_m}{12} + \frac{h^3 E_{cm}}{2(k+1)(k+2)(k+3)}. \end{aligned} \quad (9)$$

Stability equations of FGM annular spherical shells may be established by the adjacent equilibrium criterion. It is assumed that equilibrium state of the FGM annular spherical shells and under applied load is represented by displacement components u_0 , v_0 , w_0 . The state of adjacent equilibrium differs from that of stable equilibrium by u_1 , v_1 , w_1 and the total displacement components of a neighboring configuration are:

$$u = u_0 + u_1, \quad v = v_0 + v_1, \quad w = w_0 + w_1. \quad (10)$$

Similarly, the force resultants of a neighboring state are represented by:

$$\begin{aligned} N_r &= N_r^0 + N_r^1, \quad N_\theta = N_\theta^0 + N_\theta^1, \quad N_{r\theta} = N_{r\theta}^0 + N_{r\theta}^1, \\ M_r &= M_r^0 + M_r^1, \quad M_\theta = M_\theta^0 + M_\theta^1, \quad M_{r\theta} = M_{r\theta}^0 + M_{r\theta}^1. \end{aligned} \quad (11)$$

where terms with 0 subscripts represent the force and moment resultants corresponding to u_0 , v_0 , w_0 displacements and those with 1 subscripts represent the portions of increments corresponding to u_1 , v_1 , w_1 .

The equilibrium state and the state of adjacent equilibrium have satisfied all of Equations (3)–(7), subtract the corresponding equations and retain the linear terms have been obtained the stability of linear equations, which written as

$$\begin{aligned} \varepsilon_r^{01} &= \frac{\partial u_1}{\partial r} - \frac{w_1}{R}, & \chi_r^1 &= \frac{\partial^2 w_1}{\partial r^2}, \\ \varepsilon_\theta^{01} &= \frac{1}{r} \left(\frac{\partial v_1}{\partial \theta} + u_1 \right) - \frac{w_1}{R}, & \chi_\theta^1 &= \frac{1}{r} \frac{\partial w_1}{\partial r} + \frac{1}{r^2} \frac{\partial^2 w_1}{\partial \theta^2}, \\ \gamma_{r\theta}^{01} &= r \frac{\partial}{\partial r} \left(\frac{v_1}{r} \right) + \frac{1}{r} \frac{\partial u_1}{\partial \theta}, & \chi_{r\theta}^1 &= \frac{1}{r} \frac{\partial^2 w_1}{\partial r \partial \theta} - \frac{1}{r^2} \frac{\partial w_1}{\partial \theta}. \end{aligned} \quad (12)$$

the nonlinear equilibrium equations are:

$$\frac{\partial N_r^1}{\partial r} + \frac{1}{r} \frac{\partial N_{r\theta}^1}{\partial \theta} + \frac{N_r^1}{r} - \frac{N_\theta^1}{r} = 0, \quad (13)$$

$$\frac{\partial N_\theta^1}{r \partial \theta} + \frac{\partial N_{r\theta}^1}{\partial r} + \frac{2N_{r\theta}^1}{r} = 0, \quad (14)$$

$$\begin{aligned} &\frac{\partial^2 M_r^1}{\partial r^2} + \frac{2}{r} \frac{\partial M_r^1}{\partial r} + 2 \left(\frac{\partial^2 M_{r\theta}^1}{r \partial r \partial \theta} + \frac{1}{r^2} \frac{\partial M_\theta^1}{\partial \theta} \right) + \frac{1}{r^2} \frac{\partial^2 M_\theta^1}{\partial \theta^2} - \frac{1}{r} \frac{\partial M_\theta^1}{\partial r} + \frac{1}{R} (N_r^1 + N_\theta^1) \\ &+ N_r^0 \frac{\partial^2 w_1}{\partial r^2} - 2N_{r\theta}^0 \left(\frac{1}{r} \frac{\partial w_1}{\partial \theta} - \frac{\partial^2 w_1}{r \partial r \partial \theta} \right) + N_\theta^0 \left(\frac{1}{r} \frac{\partial w_1}{\partial r} + \frac{1}{r^2} \frac{\partial^2 w_1}{\partial \theta^2} \right) - k_1 w_1 + k_2 \Delta w_1 = 0. \end{aligned} \quad (15)$$

where the force and moment resultants for the state of stability are given by

$$\begin{aligned}
N_r^1 &= \left(A_{11} + \frac{E_0 A_1}{s_1} \right) \varepsilon_r^{01} + A_{12} \varepsilon_\theta^{01} - (B_{11} + C_1) \chi_r^1 - B_{12} \chi_\theta^1, \\
N_\theta^1 &= A_{12} \varepsilon_r^{01} + \left(A_{22} + \frac{E_0 A_2}{s_2} \right) \varepsilon_\theta^{01} - B_{12} \chi_r^1 - (B_{22} + C_2) \chi_\theta^1, \\
N_{r\theta}^1 &= A_{66} \gamma_{r\theta}^{01} - 2B_{66} \chi_{r\theta}^1, \\
M_r^1 &= (B_{11} + C_1) \varepsilon_r^{01} + B_{12} \varepsilon_\theta^{01} - \left(D_{11} + \frac{E_0 I_1}{s_1} \right) \chi_r^1 - D_{12} \chi_\theta^1, \\
M_\theta^1 &= B_{12} \varepsilon_r^{01} + (B_{22} + C_2) \varepsilon_\theta^{01} - D_{12} \chi_r^1 - \left(D_{22} + \frac{E_0 I_2}{s_2} \right) \chi_\theta^1, \\
M_{r\theta}^1 &= B_{66} \gamma_{r\theta}^{01} - 2D_{66} \chi_{r\theta}^1.
\end{aligned} \tag{16}$$

The considered FGM annular spherical shells are assumed to be subjected to combination of external pressure q (Pascal) uniformly distributed on the outer surface and uniformly compressive load p (Pascal) acting on the two end edges in the tangential direction to meridian of the shells. Therefore, the pre-buckling state will be symmetric and determined by membrane forces N_r^0 , N_θ^0 and $N_{r\theta}^0 = 0$. Projecting all external and internal forces acting on an element of the annular shell onto its axis of revolution yields [15]:

$$\pi r_0 p h \sin \varphi_0 + \pi r N_r^0 \sin \varphi + \int_0^\pi \int_{\varphi_0}^\varphi q R \cos \varphi \sin \varphi d\theta R d\varphi = 0, \tag{17}$$

and onto the z -direction of the shells yields:

$$\frac{N_r^0}{R_1} + \frac{N_\theta^0}{R_2} + q = 0, \tag{18}$$

in which $r_0 = R \sin \varphi_0$, $r = R \sin \varphi$, $R_1 = R_2 = R$.

Performing some calculation leads to:

$$\begin{aligned}
N_r^0 &= -\frac{qR}{2} \left(1 - \frac{\sin^2 \varphi_0}{\sin^2 \varphi} \right) - ph \frac{r_0 \sin \varphi_0}{R \sin^2 \varphi}, \\
N_\theta^0 &= -N_r^0 - Rq = -\frac{qR}{2} \left(1 + \frac{\sin^2 \varphi_0}{\sin^2 \varphi} \right) + ph \frac{r_0 \sin \varphi_0}{R \sin^2 \varphi},
\end{aligned} \tag{19}$$

and replacing $\sin \varphi_0 = \frac{r_0}{R}$, $\sin \varphi = \frac{r}{R}$, yields:

$$N_r^0 = -qR \frac{(r^2 - r_0^2)}{2r^2} - ph \frac{r_0^2}{r^2}, \quad N_\theta^0 = -qR \frac{(r^2 + r_0^2)}{2r^2} + ph \frac{r_0^2}{r^2}, \quad N_{r\theta}^0 = 0. \tag{20}$$

Substitution of Equations (12), (16) and (20) into Equations (13)–(15) gives stability equations in terms of displacement increments as:

$$l_{11}(u_1) + l_{12}(v_1) + l_{13}(w_1) = 0, \tag{21}$$

$$l_{21}(u_1) + l_{22}(v_1) + l_{23}(w_1) = 0, \tag{22}$$

$$l_{31}(u_1) + l_{32}(v_1) + l_{33}(w_1) + ql_{34}(w_1) + pl_{35}(w_1) + k_1 l_{36}(w_1) + k_2 l_{37}(w_1) = 0, \tag{23}$$

where the operators l_{ij} denote the corresponding expressions with variables. The boundary conditions in this case, are expressed by:

$$w_1 = 0, \quad M_r^1 = 0, \quad N_r^1 = 0, \quad N_{r\theta}^1 = 0, \quad \text{at } r = r_0 \tag{24}$$

From boundary conditions (24) approximate solutions for Equations (21)–(23) are assumed as:

$$\begin{aligned}
 u_1 &= U \cos \frac{m\pi(r-r_0)}{r_1-r_0} \sin(n\theta), \\
 v_1 &= V \sin \frac{m\pi(r-r_0)}{r_1-r_0} \cos(n\theta), \\
 w_1 &= W \sin \frac{m\pi(r-r_0)}{r_1-r_0} \sin(n\theta).
 \end{aligned} \tag{25}$$

where m, n are numbers of half waves in meridional and circumferential directions, respectively.

Due to $r_0 \leq r \leq r_1$ and for sake of convenience in integration, Equations (21) and (22) are multiplied by r^2 and Equation (23) by r^3 .

Subsequently, introduction of solutions (24) into obtained equations and applying Galerkin method for the resulting equation, we have:

$$\begin{aligned}
 \int_{r_0}^{r_1} \int_0^\pi R_1 \cos \frac{m\pi(r-r_0)}{r_1-r_0} \sin(n\theta) r dr d\theta &= 0, \\
 \int_{r_0}^{r_1} \int_0^\pi R_2 \sin \frac{m\pi(r-r_0)}{r_1-r_0} \cos(n\theta) r dr d\theta &= 0, \\
 \int_{r_0}^{r_1} \int_0^\pi R_3 \sin \frac{m\pi(r-r_0)}{r_1-r_0} \sin(n\theta) r dr d\theta &= 0.
 \end{aligned} \tag{26}$$

where R_1, R_2, R_3 are the left-hand sides of Equations (21)–(23) after these equations are multiplied by r^2, r^2 and r^3 , respectively, and substituted into solutions (24), we obtain the following equations:

$$\begin{aligned}
 a_{11}U + a_{12}V + a_{13}W &= 0, \\
 a_{21}U + a_{22}V + a_{23}W &= 0, \\
 a_{31}U + a_{32}V + (a_{33} + qa_{34} + pa_{35} + k_1a_{36} + k_2a_{37})W &= 0,
 \end{aligned} \tag{27}$$

where the details of coefficients a_{ij} may be found in Appendix 1.

Because the solutions (24) are nontrivial, the determinant of coefficient matrix of Equations (27) must be zero

$$\begin{vmatrix}
 a_{11} & a_{12} & a_{13} \\
 a_{21} & a_{22} & a_{23} \\
 a_{31} & a_{32} & (a_{33} + qa_{34} + pa_{35} + k_1a_{36} + k_2a_{37})
 \end{vmatrix} = 0 \tag{28}$$

Solving Equation (28) for p and q yields:

$$qa_{34} + pa_{35} = \frac{[a_{31}(a_{12}a_{23} - a_{13}a_{22}) + a_{32}(a_{13}a_{21} - a_{11}a_{23}) + (a_{33} + k_1a_{36} + k_2a_{37})(a_{11}a_{22} - a_{12}a_{21})]}{a_{12}a_{21} - a_{11}a_{22}} \tag{29}$$

Equation (29) is used for determining the buckling loads of FGM annular spherical shells under uniform compressive load, external pressure, and combined loads. For given values of the material and geometrical properties of the shells, critical buckling loads are determined by minimizing loads with respect to values of (m, n) .

By introducing parameter $\tau = \frac{p}{q}$, Equation (29) becomes:

$$q = \frac{[a_{31}(a_{12}a_{23} - a_{13}a_{22}) + a_{32}(a_{13}a_{21} - a_{11}a_{23}) + (a_{33} + k_1a_{36} + k_2a_{37})(a_{11}a_{22} - a_{12}a_{21})]}{(a_{12}a_{21} - a_{11}a_{22})(a_{34} + a_{35}\tau)} \tag{30}$$

4. Results and discussion

The linear stability of eccentrically stiffened functionally graded annular spherical shell is analyzed in this section. The shell consists of aluminum (metal) and alumina (ceramic) with the Young modulus of Aluminum $E_m = 70 \times 10^9$ Pa, and alumina $E_c = 380 \times 10^9$ Pa. The Poisson ratio is chosen to be $\nu = 0.3$ for simplicity. To illustrate the present approach, consider a FGM annular spherical shell with and without eccentric stiffeners. The geometric parameters of annular and stiffeners considered here are [15] $d_1 = d_2 = 0.002$ m, $h_1 = h_2 = 0.005$ m, $R = 2$ m. Unless otherwise specified, the inside stiffeners of the shell is ceramic-rich and the outside stiffeners is metal-rich. In case of no mention of the inside or outside stiffeners, mean was calculated for the inside stiffener of ceramic.

In which $(\frac{r_0}{R} = \frac{1}{20}, \frac{r_1}{R} = 0.5, R = 2$ m, $d_1 = d_2 = 0.002$ m, $h_1 = h_2 = 0.005$ m, $k_1 = 0, k_2 = 0, n_1 = n_2 = 30)$, $(\cdot)^*$ donate the buckling mode shape (m, n) and in case without stiffeners $A_1 = A_2 = I_1 = I_2 = 0$.

Table 1 presents the critical buckling load of shell with and without eccentric stiffeners under external pressure. The results show that the shell reinforced by the stiffeners has a great influence on stability of annular spherical shell under radial pressure. With the same input parameters, the efficiency of the stiffeners increased when the ratio R/h or volume fraction index k increased.

The effects of ratio r_0/R and r_1/R on the critical load p_{cr} and q_{cr} of the FGM annular spherical shell with and without eccentric stiffeners under compressive load and external pressure are shown in Tables 2 and 3. Obviously, the compression load and the external pressure of eccentrically stiffened FGM annular spherical shell increased when the ratio r_1/R increases and r_0/R decreases.

Tables 4 and 5 respectively indicate the influence of the elastic foundation (k_1, k_2) on the critical loads p_{cr} and q_{cr} of the eccentrically stiffened FGM annular spherical shell. Notice that with the increased value of the k_1 ($\text{N/m}^3 = (0 \times 10^7; 2.5 \times 10^7; 5 \times 10^7)$) and unchanged value of the k_2 , or the reverse, the increased value of the k_2 ($\text{N/m} = (0 \times 10^5; 2.5 \times 10^5; 5 \times 10^5)$) and unchanged value of the k_1 , the critical load values increase. In case $(k_1 = k_2 = 0)$ the value of the critical load is minimal and in case $k_1 = 5 \times 10^7 \text{ N/m}^3, k_2 = 5 \times 10^7 \text{ N/m}$ the largest.

Tables 6 and 7 show the critical loads p_{cr}, q_{cr} of the shell. Notice that the value of the critical load of the inside stiffeners are larger than the critical load of the outside stiffeners. This is understandable because the inside stiffeners of the shell is ceramic-rich and the outside stiffeners is metal-rich and the ceramic module of elasticity greater than the metal. With the same of the number stiffeners $(n_s = 30)$, the values of critical

Table 1. The critical buckling load q_{cr} (MPa) of the FGM annular spherical shell under external pressure.

k	$R/h = 800$		$R/h = 1000$		$R/h = 1200$	
	Without stiffeners	With stiffeners	Without stiffeners	With stiffeners	Without stiffeners	With stiffeners
0.2	0.523 (1, 23)	1.727 (1, 13)	0.381 (1, 16)	1.321 (1, 11)	0.122 (1, 19)	1.131 (1, 11)
1	0.334 (1, 13)	1.245 (1, 9)	0.146 (1, 14)	1.025 (1, 9)	0.076 (1, 14)	0.87 (1, 10)
5	0.109 (1, 11)	0.812 (1, 9)	0.04 (1, 11)	0.678 (1, 9)	0.03 (1, 13)	0.589 (1, 9)
10	0.03 (1, 11)	0.728 (1, 9)	0.01 (1, 9)	0.605 (1, 9)	0.01 (1, 11)	0.52 (1, 8)*

*indicates mode shape (m, n) of minimum buckling load of the stiffened shell.

Table 2. Effects of ratio r_0/R and r_1/R on the critical load p_{cr} (GPa) of the shell under compressive load ($k = 1, R/h = 1000, k_1 = 0, k_2 = 0$).

$\frac{t_0}{R}$	$r_1/R = 0.3$		$r_1/R = 0.35$		$r_1/R = 0.4$		$r_1/R = 0.45$	
	Without stiffener	With stiffeners	Without stiffener	With stiffener	Without stiffener	With stiffener	Without stiffener	With stiffener
10^{-1}	3.63 (1, 1)	5.856 (1, 1)	7.466 (1, 1)	10.940 (1, 1)	13.664 (1, 1)	18.830 (1, 1)	23.026 (1, 1)	30.391 (1, 1)
15^{-1}	9.759 (1, 1)	14.896 (1, 1)	19.426 (1, 1)	27.542 (1, 1)	34.811 (1, 1)	46.977 (1, 1)	57.81 (1, 1)	75.249 (1, 1)
20^{-1}	18.772 (1, 1)	28.208 (1, 1)	36.978 (1, 1)	51.957 (1, 1)	65.767 (1, 1)	88.281 (1, 1)	108.595 (1, 1)	140.91 (1, 1)
25^{-1}	30.723 (1, 1)	45.923 (1, 1)	60.214 (1, 1)	84.377 (1, 1)	106.675 (1, 1)	143.006 (1, 1)	175.584 (1, 1)	227.723 (1, 1)

Table 3. Effects of ratio r_0/R and r_1/R on the critical load q_{cr} (MPa) of the shell under external pressure ($k = 1$, $R/h = 1000$, $k_1 = 0$, $k_2 = 0$).

$\frac{q_0}{R}$	$r_1/R = 0.3$		$r_1/R = 0.35$		$r_1/R = 0.4$		$r_1/R = 0.45$	
	Without stiffener	With stiffeners	Without stiffener	With stiffener	Without stiffener	With stiffener	Without stiffener	With stiffener
10^{-1}	0.163 (1, 5)	0.675 (1, 5)	0.176 (1, 7)	0.782 (1, 6)	0.432 (1, 7)	0.859 (1, 7)	0.505 (1, 8)	0.895 (1, 9)
15^{-1}	0.242 (1, 5)	0.778 (1, 5)	0.384 (1, 6)	0.881 (1, 6)	0.481 (1, 7)	0.945 (1, 7)	0.545 (1, 8)	0.971 (1, 9)
20^{-1}	0.277 (1, 5)	0.836 (1, 5)	0.413 (1, 6)	0.933 (1, 6)	0.503 (1, 7)	0.988 (1, 7)	0.563 (1, 8)	1.008 (1, 9)
25^{-1}	0.297 (1, 5)	0.857 (1, 5)	0.429 (1, 6)	0.964 (1, 6)	0.516 (1, 7)	1.014 (1, 7)	0.573 (1, 8)	1.03 (1, 9)

load in the case of ring-stiffened shell is the largest of the three cases of stiffener arrangement (stringer, ring, orthogonal).

The effect of stiffener number on critical loads p_{cr} , q_{cr} is shown in Tables 8, 9 and Figures 2, 3.

Table 4. Influences of elastic foundation on the critical load p_{cr} (GPa) of the shell under compressive load ($R = 2$, $k = 1$, $R/h = 1000$, $r_1/R = 0.3$, $R/r_0 = 20$).

k_2 (N/m) k_1 (N/m ³)	0×10^5	1×10^5	2.5×10^5	5×10^5
0×10^7	28.208 (1, 1)	29.7972 (1, 1)	32.1801 (1, 1)	36.1518 (1, 1)
1×10^7	31.1018 (1, 1)	32.6904 (1, 1)	35.0734 (1, 1)	39.0450 (1, 1)
2.5×10^7	35.4416 (1, 1)	37.0303 (1, 1)	39.4133 (1, 1)	43.3849 (1, 1)
5×10^7	42.6748 (1, 1)	44.2635 (1, 1)	46.6464 (1, 1)	50.6181 (1, 1)

Table 5. Influences of elastic foundation on the critical load q_{cr} (MN) of the shell external pressure ($k = 1$, $R/h = 1000$, $r_1/R = 0.3$, $R/r_0 = 20$).

k_2 (N/m) k_1 (N/m ³)	0×10^5	1×10^5	2.5×10^5	5×10^5
0×10^7	0.8361 (1, 5)	0.9316 (1, 5)	1.0748 (1, 5)	1.3135 (1, 5)
1×10^7	0.8832 (1, 5)	0.9786 (1, 5)	1.1218 (1, 5)	1.3605 (1, 5)
2.5×10^7	0.9537 (1, 5)	1.0491 (1, 5)	1.1924 (1, 5)	1.4311 (1, 5)
5×10^7	1.0712 (1, 5)	1.1667 (1, 5)	1.3099 (1, 5)	1.5486 (1, 5)

Table 6. The effect of stiffener arrangement on critical load p_{cr} (GPa), ($k = 1$, $R/h = 1000$, $r_1/R = 0.3$, $R/r_0 = 20$).

p_{cr} (textGPa)	Outside	Inside
Un-stiffened	18.7728 (1, 1)	18.7728 (1, 1)
Stringer ($n_1 = 30$)	20.3599 (1, 1)	20.9102 (1, 1)
Ring ($n_2 = 30$)	21.7343 (1, 1)	27.6560 (1, 1)
Orthogonal ($n_1 = n_2 = 15$)	21.0549 (1, 1)	24.4792 (1, 1)

Table 7. Effect of stiffeners arrangement on critical load q_{cr} (MN), ($k = 1$, $R/h = 1000$, $r_1/R = 0.3$, $R/r_0 = 20$, $k_1 = 0$, $k_2 = 0$).

q_{cr} (MN)	Outside	Inside
Un-stiffened	0.2772 (1, 5)	0.2772 (1, 5)
Stringer ($n_1 = 30$)	0.6979 (1, 4)	0.7007 (1, 4)
Ring ($n_2 = 30$)	0.7261 (1, 4)	0.8259 (1, 4)
Orthogonal ($n_1 = n_2 = 15$)	0.7124 (1, 4)	0.7704 (1, 4)

Both tables show that the value of the critical load increases when the stiffener number increased and vice versa. The increasing trend of critical load curve with increasing the stiffener number can be seen in figures 2 and 3.

Table 8. Effect of stiffeners number on critical load p_{cr} (GPa), ($k = 1, R/h = 1000, r_1/R = 0.3, R/r_0 = 20, k_1 = 0, k_2 = 0$).

Stiffener number ($n_1 = n_2$)	p_{cr} (GPa)	
	Outside	Inside
10	20.5055 (1, 1)	21.7095 (1, 1)
20	20.7814 (1, 1)	23.1253 (1, 1)
30	21.0549 (1, 1)	24.4792 (1, 1)
40	21.3261 (1, 1)	25.7752 (1, 1)
50	21.5949 (1, 1)	27.0172 (1, 1)

Table 9. Effect of stiffener number on critical load q_{cr} (MN), ($k = 1, R/h = 1000, r_1/R = 0.3, R/r_0 = 20, k_1 = 0, k_2 = 0$).

Stiffener number ($n_1 = n_2$)	q_{cr} (MN)	
	Outside	Inside
10	0.7024 (1, 4)	0.7240 (1, 4)
20	0.7074 (1, 4)	0.7483 (1, 4)
30	0.7124 (1, 4)	0.7704 (1, 4)
40	0.7173 (1, 4)	0.7909 (1, 4)
50	0.7220 (1, 4)	0.8100 (1, 4)

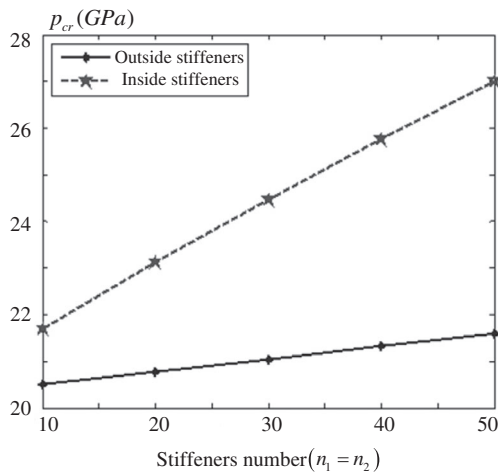


Figure 2. Effect of stiffeners number on critical load p_{cr} (GPa).

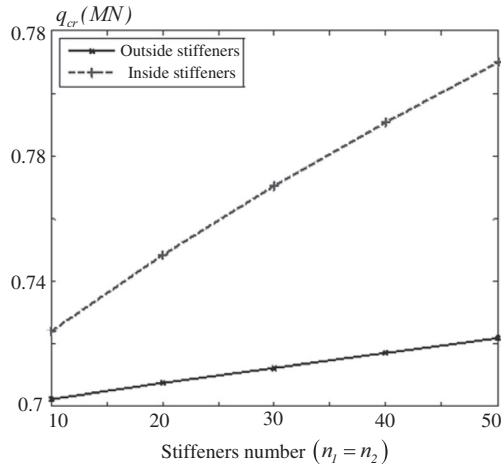


Figure 3. Effect of stiffener number on critical load q_{cr} (MN).

5. Concluding remarks

The present paper aims to propose a linear analysis of eccentrically stiffened FGM annular spherical shell on elastic foundations under uniform external pressure and compressive load. Approximate solutions are assumed to satisfy the simply supported boundary condition and Galerkin method is applied to obtain closed-form solutions of bifurcation type of linear stability. The effects of material, geometrical properties, elastic foundations, combination of external pressure and stiffener arrangement, stiffener number on the linear stability of eccentrically stiffened FGM annular spherical shell are analyzed and discussed.

Acknowledgement

This work support by Vietnam National University, Hanoi. The author are grateful for this support.

Funding

Vietnam National University, Hanoi.

References

- [1] Najafzadeh MM, Hasani A, Khazaeinejad P. Mechanical stability of functionally graded stiffened cylindrical shells. *Appl. Math. Model.* **2009**;33:1151–1157.
- [2] Bich DH, Nam VH, Phuong NT. Nonlinear post-buckling of eccentrically stiffened functionally graded plates and shallow shells. *Vietnam J. Mech.* **2011**;33:131–147.
- [3] Bich DH, Dung DV, Nam VH. Nonlinear dynamical analysis of eccentrically stiffened functionally graded cylindrical panels. *Compos. Struct.* **2012**;94:2465–2473.
- [4] Dung DV, Hoa LK. Nonlinear buckling and post-buckling analysis of eccentrically stiffened functionally graded circular cylindrical shells under external pressure. *Thin-Walled Struct.* **2013**;63:117–124.
- [5] Dung DV, Hoa LK. Research on nonlinear torsional buckling and post-buckling of eccentrically stiffened functionally graded thin circular cylindrical shells. *J. Compos. Struct.* **2013**;51:300–309.
- [6] Duc ND. Nonlinear dynamic response of imperfect eccentrically stiffened FGM double curved shallow shells on elastic foundation. *Compos. Struct.* **2013**;102:306–314.

- [7] Duc ND, Quan TQ. Nonlinear postbuckling of imperfect eccentrically stiffened P-FGM double curved thin shallow shells on elastic foundations in thermal environments. *Compos. Struct.* **2013**;106:590–600.
- [8] Duc ND, Quan TQ. Nonlinear dynamic analysis of imperfect FGM double curved thin shallow shells with temperature-dependent properties on elastic foundation. *J. Vib. Control.* **2013**;21:1340–1362.
- [9] Duc ND, Quan TQ. Nonlinear postbuckling of imperfect doubly curved thin shallow FGM shells resting on elastic foundations and subjected to mechanical loads. *Mech. Compos. Mater.* **2013**;49:493–506.
- [10] Duc ND, Thang TP. Nonlinear buckling of imperfect eccentrically stiffened metal-ceramic-metal S-FGM thin circular cylindrical shells with temperature-dependent properties in thermal environments. *Int. J. Mech. Sci.* **2014**;81:17–25.
- [11] Duc ND, Thang TP. Nonlinear response of imperfect eccentrically stiffened ceramic–metal–ceramic FGM thin circular cylindrical shells surrounded on elastic foundations and subjected to axial compression. *Compos. Struct.* **2014**;110:200–206.
- [12] Alwar RS, Narasimhan MC. Axisymmetric non-linear analysis of laminated orthotropic annular spherical shells. *Int. J. Non Linear Mech.* **1992**;27:611–622.
- [13] Chih-Ping Wu, Tsai Y-H. The asymptotic DQ solutions of functionally graded annular spherical shells. *Eur. J. Mech. A. Solids.* **2004**;23:283–299.
- [14] Anh VTT, Bich DH, Duc ND. Nonlinear buckling analysis of thin FGM annular spherical shells on elastic foundations under external pressure and thermal loads. *Eur. J. Mech. A. Solids.* **2015**;50:28–38.
- [15] Bich DH, Phuong NT. Buckling analysis of functionally graded annular spherical shells and segments subjected to mechanical loads. *VNU J. Math. Phys.* **2013**;29:14–31.

Appendix 1.

$$a_{11} = \frac{n^2 \pi A_{66} (r_0^2 - r_1^2)}{8} + \frac{\pi^2 m^2 [3\pi A_{11} (r_1^3 + r_0^2 r_1 + r_0 r_1^2 + r_0^3) + 2E_0 A_1 n_1 (r_1^2 + r_0 r_1 + r_0^2)]}{48(-r_1 + r_0)} + \frac{\pi (r_0^2 - r_1^2) (A_{11} + 2A_{22})}{16} + \frac{\pi E_0 A_2 (r_0^2 - r_1^2)}{8s_2},$$

$$a_{12} = -\frac{1}{12} \pi^2 mn (r_1^2 + r_0 r_1 + r_0^2) (A_{12} + A_{66}) - \frac{n(-r_1 + r_0)^2 (A_{12} + 2A_{66} + A_{22})}{8m} - \frac{n(-r_1 + r_0)^2 E_0 A_2}{8ms_2},$$

$$a_{13} = \frac{n^2 \pi^2 m (r_1 + r_0) (B_{12} + 2B_{66})}{8} + \frac{\pi^3 m^3 [3\pi B_{11} (r_1^3 + r_0^2 r_1 + r_0 r_1^2 + r_0^3) + 2E_0 A_1 z_1 n_1 (r_1^2 + r_0 r_1 + r_0^2)]}{48(-r_1 + r_0)^2} + \frac{m\pi [3\pi (r_1^3 + r_0^2 r_1 + r_0 r_1^2 + r_0^3) (A_{11} + A_{12}) + 2E_0 A_1 n_1 (r_1^2 + r_0 r_1 + r_0^2) - 3\pi R (2B_{22} + 2C_2 + B_{11}) (r_1 + r_0)]}{48R} + \frac{(r_1 + r_0) (-r_1 + r_0)^2 (2A_{22} + A_{11} + 3A_{12})}{16} - \frac{(r_1 + r_0) (-r_1 + r_0)^2 E_0 A_2}{8mR s_2},$$

$$a_{21} = -\frac{\pi^2 mn (r_1^2 + r_0 r_1 + r_0^2) (A_{12} + A_{66})}{12} + \frac{n(-r_1 + r_0)^2 (A_{12} - A_{22})}{8m} - \frac{nE_0 A_2 (-r_1 + r_0)^2}{8ms_2},$$

$$a_{22} = \frac{n^2 \pi (r_0^2 - r_1^2) A_{22}}{8} + \frac{\pi^3 m^2 (r_1 + r_0) (r_0^2 + r_1^2)}{16(-r_1 + r_0)} + \frac{\pi A_{66} (r_0^2 - r_1^2)}{16} + \frac{n^2 \pi E_0 A_2 (r_0^2 - r_1^2)}{8s_2},$$

$$\begin{aligned}
a_{23} = & -\frac{\pi n^3(-r_1+r_0)(B_{22}+C_2)}{4} - \frac{m^2 n \pi^3 (r_1^2+r_0 r_1+r_0^2)(B_{12}+2B_{66})}{12(-r_1+r_0)} \\
& - \frac{n(-r_1+r_0)^3(A_{22}+A_{12})}{8\pi m^2 R} + \frac{\pi n E_0 A_2 (r_0^3-r_1^3)}{12 R s_2} + \frac{-n E_0 A_2 (-r_1+r_0)^3}{8\pi m^2 R s_2} \\
& + \frac{\pi n(-r_1+r_0)[2(A_{22}+A_{12})(r_1^2+r_0 r_1+r_0^2)+3R(B_{12}-B_{22}-C_2)]}{24R}, \\
a_{31} = & \frac{m n^2 \pi^2}{12}(B_{12}+2B_{66})(r_1^2+r_0 r_1+r_0^2) - \frac{n^2(-r_1+r_0)^2}{8m}(B_{12}+2B_{66}-B_{22}-C_2) \\
& - \frac{E_0 A_2 (-r_1+r_0)^2 (r_1^2+r_0 r_1+r_0^2)}{8m R s_2} \\
& + \frac{m \pi}{160R} \left[-8\pi(A_{11}+A_{12})(r_0^4+r_0^3 r_1+r_0^2 r_1^2+r_0 r_1^3+r_1^4) - 5E_0 A_1 n_1 (r_1^3+r_0^2 r_1+r_0 r_1^2+r_0^3) \right] \\
& + \frac{(-r_1+r_0)^2 [4\pi(r_1^2+r_0 r_1+r_0^2)(2A_{11}+A_{12}-A_{22})+3E_0 A_1 n_1 (r_1+r_0)-6\pi R B_{12}]}{32\pi m R} \\
& - \frac{3(-r_1+r_0)^4 (2A_{11}+A_{12}-A_{22})}{16\pi^2 m^3 R} \\
& + \frac{\pi^3 m^3 [8\pi B_{11}(r_0^4+r_0^3 r_1+r_0^2 r_1^2+r_0 r_1^3+r_1^4)+5E_0 A_1 n_1 z_1 (r_1^3+r_0^2 r_1+r_0 r_1^2+r_0^3)]}{160(-r_1+r_0)^2} \\
& + \frac{3E_0 A_2 (-r_1+r_0)^4}{16\pi^2 m^3 R s_2}, \\
a_{32} = & \frac{-\pi n^3}{8}(r_0^2-r_1^2)(B_{22}+C_2) - \frac{\pi^3 n m^2 (r_1+r_0)(r_0^2+r_1^2)(B_{12}+2B_{66})}{16(-r_1+r_0)} \\
& - \frac{n(r_0^2-r_1^2)(-r_1+r_0)^2 (A_{12}+A_{22})}{16R\pi m^2} \\
& + \frac{n\pi(r_0^2-r_1^2)[(A_{12}+A_{22})(r_0^2+r_1^2)+3R(B_{12}+2B_{66})]}{16R} + \frac{\pi n E_0 A_2 (r_0^4-r_1^4)}{16R s_2} \\
& - \frac{3n E_0 A_2 (r_0^2-r_1^2)(-r_1+r_0)^2}{16R\pi m^2 s_2}, \\
a_{33} = & \frac{m^2 n^2 \pi^3 (r_0^2+r_0 r_1+r_1^2)(2D_{66}+D_{12})}{6(-r_1+r_0)} + \frac{n^2(-r_1+r_0)^3 (B_{12}+B_{22}+C_2)}{4\pi m^2 R} + \frac{n^4 \pi D_{22}(-r_1+r_0)}{4} \\
& + \frac{(-r_1+r_0)^5 E_0 A_2}{8\pi^3 m^4 R^2 s_2} + \frac{\pi E_0 A_2 (-r_1+r_0)(r_1^4+r_0 r_1^3+r_0^2 r_1^2+r_0^3 r_1+r_0^4)}{20R^2 s_2} + \frac{3(-r_1+r_0)^5 (A_{11}+A_{22}+2A_{12})}{8\pi^3 m^4 R^2} \\
& + \frac{E_0 A_2 (r_0^2+r_0 r_1+r_1^2)(-r_1+r_0)^3}{4\pi m^2 R^2 s_2} + \frac{\pi n^2 (-r_1+r_0)}{24R} \left[4(B_{12}+B_{22}+C_2)(r_0^2+r_0 r_1+r_1^2) \right. \\
& \left. + 3R(4D_{66}+8D_{12}-D_{22}) \right] \\
& + \frac{\pi^4 m^4}{160(-r_1+r_0)^3} \left[8\pi D_{11}(r_0^4+r_0 r_1^3+r_1^4+r_0^3 r_1+r_0^2 r_1^2) \right. \\
& \left. + 5E_0 I_1 n_1 (r_0^3+r_0 r_1^2+r_0^2 r_1+r_1^3) \right] \\
& + \frac{\pi^2 m^2}{160R(-r_1+r_0)} \left[10E_0 A_1 z_1 n_1 (r_0^3+r_0 r_1^2+r_0^2 r_1+r_1^3) - 20\pi R D_{12}(r_0^2+r_0 r_1+r_1^2) \right. \\
& \left. + 16\pi(B_{12}+B_{11})(r_0^4+r_0 r_1^3+r_1^4+r_0^3 r_1+r_0^2 r_1^2) - 5R n_1 E_0 I_1 (r_1+r_0) \right] \\
& + \frac{(2n^2+1)n^2 \pi E_0 I_2 (-r_1+r_0)}{4s_2} \\
& + \frac{(-r_1+r_0)}{160R^2} \left[20\pi R(B_{12}-B_{22}-C_2+2B_{11})(r_0^2+r_0 r_1+r_1^2) + 5E_0 A_1 n_1 (r_0^3+r_0 r_1^2+r_0^2 r_1+r_1^3) \right. \\
& \left. + 8\pi(A_{11}+A_{22}+2A_{12})(r_0^4+r_0 r_1^3+r_1^4+r_0^3 r_1+r_0^2 r_1^2) + 10E_0 A_1 n_1 z_1 R(r_1+r_0) - 30\pi R^2 D_{12} \right] \\
& + \frac{(-r_1+r_0)^3}{32\pi^2 m^2 R^2} \left[8\pi(A_{11}+A_{22}+2A_{12})(r_0^2+r_0 r_1+r_1^2) \right. \\
& \left. + 6\pi R(B_{12}-B_{22}-C_2+2B_{11}) + 3E_0 A_1 n_1 (r_1+r_0) \right],
\end{aligned}$$

$$\begin{aligned}
a_{34} &= -\frac{\pi R n^2 (-r_1 + r_0)(r_1^2 + r_0 r_1 + 4r_0^2)}{24} - \frac{R(2n^2 + 3)(-r_1 + r_0)^3}{32^2 \pi} \\
&\quad + \frac{\pi^3 R m^2 (3r_1^3 + 4r_0^2 r_1 + 6r_0 r_1^2 + 2r_0^3)}{120} + -\frac{R\pi(-r_1 + r_0)(-r_1^2 - r_0 r_1 + r_0^2)}{16}, \\
a_{35} &= \frac{hr_0^2 \pi (-r_1 + r_0)(n^2 + 1)}{4} - \frac{hr_0^2 m^2 \pi^3 (r_0^2 + r_0 r_1 + r_1^2)}{12(-r_1 + r_0)}, \\
a_{36} &= \frac{3(-r_1 + r_0)^5}{8m^4 \pi^3} - \frac{(-r_1 + r_0)^2 (r_0^3 - r_1^3)}{4m^2 \pi} + \frac{\pi(-r_1 + r_0)^5}{20}, \\
a_{37} &= \frac{\pi(r_0^3 - r_1^3)}{8} - \frac{m^2 \pi^3 (r_0^4 + r_0^2 r_1^2 + r_0 r_1^3 + r_0^3 r_1 + r_1^4)}{20(-r_1 + r_0)} \\
&\quad - \frac{(2n^2 + 3)(-r_1 + r_0)^3}{16\pi m^2} - \frac{\pi n^2 (r_0^3 - r_1^3)}{12}.
\end{aligned}$$